Three-Dimensional Block Copolymer Nanostructures by the Solvent-Annealing-Induced Wetting in Anodic Aluminum Oxide Templates

Chiang-Jui Chu, Pei-Yun Chung, Mu-Huan Chi, Yi-Huei Kao, Jiun-Tai Chen*

Block copolymers have been extensively studied over the last few decades because they can self-assemble into well-ordered nanoscale structures. The morphologies of block copolymers in confined geometries, however, are still not fully understood. In this work, the fabrication and morphologies of three-dimensional polystyrene-*block*-polydimethylsiloxane (PS-*b*-PDMS) nanostructures confined in the nanopores of anodic aluminum oxide (AAO) templates are studied. It is discovered that the block copolymers can wet the nanopores using a novel solvent-annealing-induced nanowetting in templates (SAINT) method. The unique advantage of this method is that the problem of thermal degradation can be avoided. In addition, the morphologies of PS-*b*-PDMS nanostructures can be controlled by changing the wetting conditions. Different solvents are used as the annealing solvent, including toluene, hexane, and a co-solvent of toluene and hexane. When the block copolymer wets the nanopores in toluene vapors, a perpendicular morphology is observed. When the block copolymer wets the nanopores in co-solvent vapors (toluene/hexane = 3:2), unusual circular and helical morphologies are obtained. These three-dimensional nanostructures can serve as naontemplates for refilling with other functional materials, such as Au, Ag, ZnO, and TiO_2.

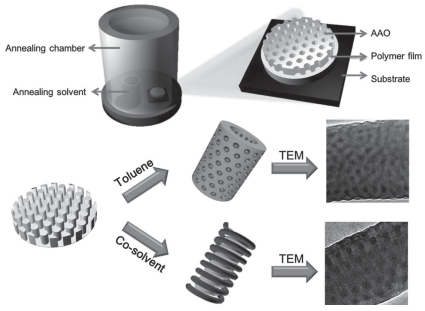

1. Introduction

Block copolymers comprising two or more polymer blocks have been extensively studied over the last few decades because they can self-assemble into well-ordered nanoscale structures.[1,2] Different applications based on block copolymers have been developed, such as nanolithography, photovoltaics, and drug delivery.[3–6] Depending on the volume fraction and chemical nature of the blocks, various morphologies can be formed in block copolymers, including lamellae, cylinders, spheres, and gyroids.[7,8] With different etching resistances to solvent or irradiation, one of the polymer blocks can be removed selectively and nanoporous patterns can be formed. The requirements of ideal nanofabrication using block copolymers include high resolution (≈10 nm), large-area manufacturing, and low defect densities.

Most studies on the morphologies of block copolymers focus on non-confined conditions, in which bulk samples or thin films of block copolymers are investigated.

C.-J. Chu, P.-Y. Chung, M.-H. Chi, Y.-H. Kao, Prof. J.-T. Chen
Department of Applied Chemistry, National Chiao Tung University, Hsinchu, Taiwan 30050, Republic of China
E-mail: jtchen@mail.nctu.edu.tw

DOI: 10.1002/marc.201400222

Recently, there have been increasing interests in the studies of block copolymers in confined geometries.[9–12] By placing the copolymers molecules in a cylindrical pore geometry, the morphologies are influenced by both the commensurability and curvature.[13] The unusual morphologies imposed by the confinement effect expand the scope of applications using block copolymers, leading to devices with smaller sizes and new functions. For example, Russell and co-workers[13–17] studied the phase separation of polystyrene-*block*-polybutadiene (PS-*b*-PBD) confined in the nanopores of anodic aluminum oxide (AAO) templates. Single-helices or double-helices structures, which are not observed in the bulk state, can be obtained. Steinhart et al. also studied the phase separation of polystyrene-*block*-poly(methyl methacrylate) (PS-*b*-PMMA) in the nanopores of AAO templates. Mesoporous PS fibers can be fabricated by removing the sacrificial PMMA block selectively.[18,19]

The most commonly used template to study the block copolymers morphologies in cylindrical confinement is the AAO template, which can be prepared by the chemical anodization process of an aluminum foil.[20] Masuda and Fukuda[21] developed a second anodization process to prepare well-ordered AAO templates with hexagonally packed nanopores. The pore size, pore-to-pore distance, and pore length of the AAO template can be controlled by the anodization conditions, such as the electrolyte type, electrolyte concentration, anodization voltage, anodization temperature, and anodization time.[22,23]

In order to study the morphologies of block copolymers confined in porous templates, it is critical to control the ways of introducing the polymer chains into the nanopores. In general, there are two main methods to introduce block copolymers into the nanopores of the templates. They are the melt method and the solution method. In the melt method, polymer films or powders are placed above or under porous templates. Steinhart et al.[24,25] pioneered the melt method by placing polymers on pore arrays at temperatures above the glass transition temperatures or the melting temperatures. Amorphous or semicrystalline polymer nanotubes have been prepared by this method. Russell and co-workers[26] later studied the wetting transition of polymer melts with different molecular weights using the melt method. Polystyrene nanotubes or nanorods can be generated, depending on whether the polymer melts are in the complete wetting regime (spreading coefficient $S > 0$) or the partial wetting regime (spreading coefficient $S < 0$).[27] It has to be noted that a solvent is not involved in the melt method.

In the solution method, polymers are first dissolved in a suitable solvent and the polymer solution wet the nanopores of the templates via capillary force. Polymer nanotubes are usually obtained after the evaporation of the solvent, and the wall thicknesses of the resultant polymer nanotubes can be controlled by the polymer concentration. Using the solution method, homopolymer and block copolymer nanotubes have been prepared.[28–30] Rayleigh-instability-type transformations have also been observed by thermally annealing the polymer nanotubes prepared by the solution method.[31–33]

Both the melt method and the solution method are commonly used in fabricating 1D polymer nanostructures using porous templates. But there are some disadvantages for these two methods. For the melt method, the main disadvantage is the problem of thermal degradation after annealing at high temperatures. Therefore, the properties of the nanostructures can be affected, limiting the possible applications of the polymer nanostructures. For the solution method, there are usually unwanted polymer films outside the nanopores of the templates after the evaporation of the solvent. The removing processes of the outer films are usually problematic and can affect the morphologies and properties of the nanostructures in the nanopores.

To overcome the limitations of the traditional template wetting methods, it is desirable to develop simple and reliable methods for the preparation of template-based polymer nanostructures. Recently, Ho and co-workers,[34] Jin and co-workers,[35] and Chen and co-workers[36] developed the solvent-annealing-induced wetting method using porous templates, in which the polymer chains wet the pores in the presence of solvent vapors. This method is also referred to as the solvent-annealing-induced nanowetting in templates (SAINT) method.[36] Annealing at high temperatures is avoided in the SAINT method, and the problem of thermal degradation is resolved. For homopolymers, we discovered that the morphologies of the resultant polymer nanostructures can be controlled by the wetting conditions (complete wetting or partial wetting) of the polymer chains during the solvent-annealing process.[36] For example, PMMA ($\bar{M}_w$ = 68.5 kg mol^{-1}) nanotubes are formed in the nanopores of AAO templates by annealing a PMMA film in toluene vapors, where the swollen PMMA chains are in the complete wetting regime (spreading coefficient $S > 0$). On the contrary, PMMA nanorods are formed in the nanopores of AAO templates by annealing a PMMA film in dimethylformamide (DMF) vapors, where the swollen PMMA chains are in the partial wetting regime (spreading coefficient $S < 0$).[36] Despite these works, it is still unclear whether nanostructures from more complex polymer systems, such as block copolymers, can be fabricated by the SAINT method. Even so, it is also necessary to understand how the morphologies of the fabricated nanostructures can be controlled by the experimental conditions during the solvent-annealing process.

Here, we study the formation of block copolymer nanostructures using the SAINT method and investigate the

effects of the solvent-annealing conditions on the morphologies of the block copolymer nanostructures. While the polymer chains are wetting the nanopores of the templates, the block copolymer chains can achieve more equilibrium morphologies. Different from the melt method, the Flory–Huggins interaction parameter (χ) between the two blocks is also affected by the solvent during the annealing process.[37] The volume fractions of the two blocks are also changed due to the different degree of swelling of polymer chains in the solvent vapors.[38]

The block copolymer used in this work is polystyrene-*block*-polydimethylsiloxane (PS-*b*-PDMS). This polymer has been suggested as a promising candidate for nanolithography because it can self-assemble into microdomain patterns with large correlation lengths and low defect densities.[39] PS-*b*-PDMS has a high Flory–Huggins interaction parameter (χ = 0.27) at room temperature, much higher than those from other common block copolymers, such as PS-*b*-PMMA (χ = 0.04–0.06) and polystyrene-*block*-polyferrocenylsilane (PS-*b*-PFS, χ = 0.08).[40] The high χ value of PS-*b*-PDMS allows the fabrication of sub-10 nm patterns.[41] Because of the silicon-containing PDMS block, there is a large etching selectivity between PS and PDMS and one of the blocks can be removed selectively using suitable etching methods, such as O_2 plasma.

To understand the relationship between the annealing solvent and the resultant morphologies of the PS-*b*-PDMS nanostructures, three different solvents are used, including toluene, hexane, and a mixture of solvent (toluene and hexane). We find that PS-*b*-PDMS nanostructures can be successfully fabricated using the SAINT method. More importantly, the morphologies of the PS-*b*-PDMS nanostructures can be controlled using different solvents. The results presented in this work open a new avenue for constructing 3D block copolymer nanostructures with controllable morphologies, which are not accessible by other means.

2. Experimental Section

2.1. Materials

Polystyrene-*block*-polydimethylsiloxane was purchased from Polymer Source Inc. with a molecular weight of (31-*b*-14.5) kg mol^{-1} and a polydispersity index (PDI) of 1.15. Toluene and hexane were obtained from TEDIA. Acetone, ethanol, and isopropyl alcohol were purchased from Echo Chemical. Ammonium hydroxide (NH_4OH) was obtained from Merck. Hydrogen fluoride (HF) was obtained from Union Chemicals. Deionized water was obtained from Milli-Q system. AAO templates (pore diameter ≈150–400 nm, thickness ≈60 μm) were obtained from Whatman. Polycarbonate filters (VCTP, pore size ≈0.1 μm) were purchased from Millipore. Four-inch Si (1 0 0) wafers were obtained from Guv Team International Co., Ltd.

2.2. Fabrication of PS-*b*-PDMS Nanostructures

A 1 wt% PS-*b*-PDMS solution in toluene was first prepared. Then, the polymer solution (50 μL) was dropped onto a silicon wafer. After the solvent was evaporated, the polymer film on the silicon wafer was further dried by a vacuum pump. Subsequently, an AAO template was placed on top of the polymer film. The sample was then moved to a glass chamber, which contains an open bottle of the annealing solvent such as toluene or hexane. The chamber was sealed with a parafilm to prevent the solvent from leakage. The sample-containing chamber was then placed in an oven with a constant temperature of 30 °C to control the vapor pressure of the solvent. The solvent-annealing process was carried out for 24 h.

After the solvent-annealing process, the sample was taken out from the glass chamber and dried by a vacuum pump. The sample was then immersed into a 5 wt% NH_4OH solution for 6 h to dissolve the AAO template selectively. Finally, the sample was filtered using a polycarbonate membrane and washed with deionized water for several times.

For the selective removal process to prepare porous PS nanostructures, the sample was also subjected to the solvent-annealing process. After the sample was taken out from the glass chamber, the AAO-containing sample was immersed into a 48 wt% HF solution for 10 s. Finally, the sample was washed with deionized water for several times and filtered using a polycarbonate membrane.

2.3. Structure Analysis and Characterization

An atomic force microscope (AFM, Veeco diInnova) under a tapping mode was used to study the surface morphology of the block copolymer thin films. The block copolymer nanostructures were characterized by a scanning electron microscope (SEM; JEOL JSM-7401) at an acceleration voltage of 5 kV. Before the SEM measurement, the samples were dried by a vacuum pump and coated with 4 nm of platinum. The block copolymer samples were also characterized with a transmission electron microscope (TEM; JEOL JEM-2100) with an acceleration voltage of 200 kV. Before the TEM measurement, the samples were placed onto copper grids coated with Formvar or carbon.

3. Results and Discussion

In this work, PS-*b*-PDMS block copolymers with a molecular weight of $\bar{M}_w$ = 45.5 kg mol^{-1} and a PDMS volume fraction of 33.5% are used. We first examine the morphologies of PS-*b*-PDMS thin films by spin-coating a 1 wt% PS-*b*-PDMS solution in toluene on a silicon substrate. As shown in the AFM images (Figure S1, Supporting Information), cylindrical PDMS domains parallel to the silicon substrate are observed, due to the lower surface tension of the PDMS block and the preferential swelling of the solvent.[42]

The fabrication process of PS-*b*-PDMS nanostructures using the SAINT method is illustrated in Scheme 1. A PS-*b*-PDMS film is first prepared by drop-casting a PS-*b*-PDMS

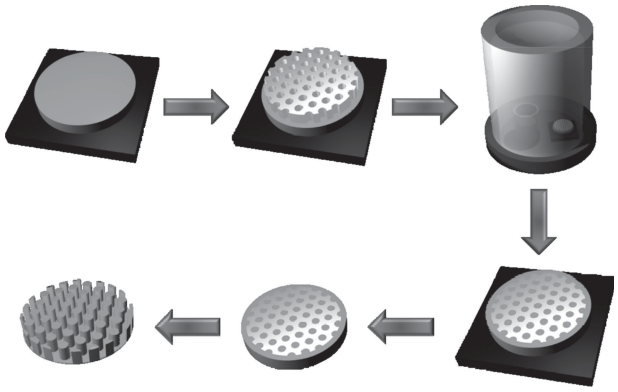

Scheme 1. Schematic illustration of the fabrication process to prepare the block copolymer nanostructures. The sample is annealed in a glass chamber, which contains an open bottle of the annealing solvent. After the annealing process, the AAO template is dissolved selectively by a NH_4OH solution to release the block copolymer nanostructures.

solution in toluene onto a silicon substrate, followed by a drying process. Subsequently, an AAO membrane is placed on top of the PS-*b*-PDMS film. The whole sample is then annealed in a sealed chamber with solvent vapors for different periods of time. The solvent-annealing process is carried out at a temperature of 30 °C to maintain a constant solvent vapor pressure. After the polymer chains are introduced into the nanopores of the AAO template by the SAINT method, the template is removed selectively by $NH_4OH_{(aq)}$ to release the PS-*b*-PDMS nanostructures.

Solvent annealing has been commonly employed to increase the chain flexibility and to facilitate the self-assembly of the block copolymers. To study the effect of solvent annealing under different solvent vapors, the Hildebrand solubility parameters (δ) of the solvents and polymers are considered. The Hildebrand solubility parameter is defined as the square root of the cohesive energy density and often used to predict the polymer dissolution and swelling in solvents.[43] Polymers are soluble and easier to be swelled in solvents with similar solubility parameters. The solubility parameters (δ) of PS, PDMS, toluene, and hexane are 18.5, 15.5, 18.2, and 14.9 $(MPa)^{1/2}$, respectively.[44] Therefore, toluene is a better solvent for the PS block and hexane is a better solvent for the PDMS block. By using toluene, hexane, or the co-solvent of toluene and hexane, the morphologies of the PS-*b*-PDMS nanostructures can be controlled.

During the solvent-annealing process, the solvent vapors can have several effects on the morphologies of the block copolymers. As the volume fraction of the solvent (φ_s) in the polymer film increases, the effective Flory–Huggins interaction parameter (χ_{eff}) decreases, due to the screening effect of the solvent.[37,45,46] The relationship between χ_{eff} and φ_s can be described as the following[46]

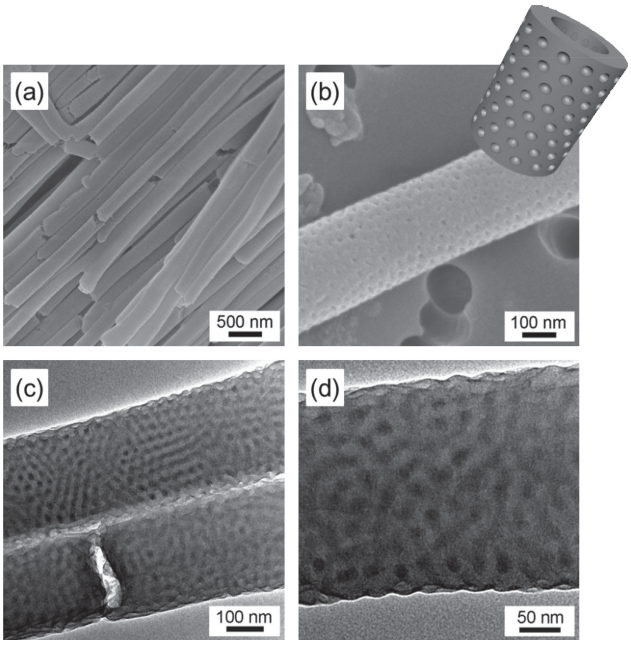

Figure 1. a,b) SEM images of PS-*b*-PDMS nanostructures: a) lower magnification and b) higher magnification. c,d) TEM images of PS-*b*-PDMS nanostructures: c) lower magnification and d) higher magnification. The samples are prepared by annealing the block copolymer films in toluene vapors for 24 h.

$$\chi_{eff} = \chi(1-\phi_s) \quad (1)$$

The equilibrium domain spacing is also affected because of the change of the effective segregation strength, $\chi_{eff} N$, where N is the total number of segments in the polymer chain.

Different from the traditional melt and solution method to introduce block polymers into nanopores, it is questionable whether the block copolymers can wet the nanopores in the presence of solvent vapors. We examine this question first by using toluene as the annealing solvent and find that PS-*b*-PDMS block copolymers can be introduced into the nanopores of AAO templates successfully, as shown in the SEM images (Figure 1a,b). The dimpled surfaces of the PS-*b*-PDMS nanostructures indicate the microphase separation of the PS and PDMS blocks. The cylindrical PDMS domains are perpendicular to the AAO walls (the perpendicular morphology). The perpendicular morphology of the PS-*b*-PDMS can be further examining by TEM, as shown in Figure 1c,d. Due to the existence of Si in the PDMS block, there is a clear contrast between the PS and PDMS domains. Therefore, the microphase separation of the block copolymers can be resolved without any staining process. The PDMS block appears darker than the PS block in the TEM images, due to the higher electron density of PDMS.

Then, hexane is used as the annealing solvent for wetting the AAO template with PS-*b*-PDMS block copolymers.

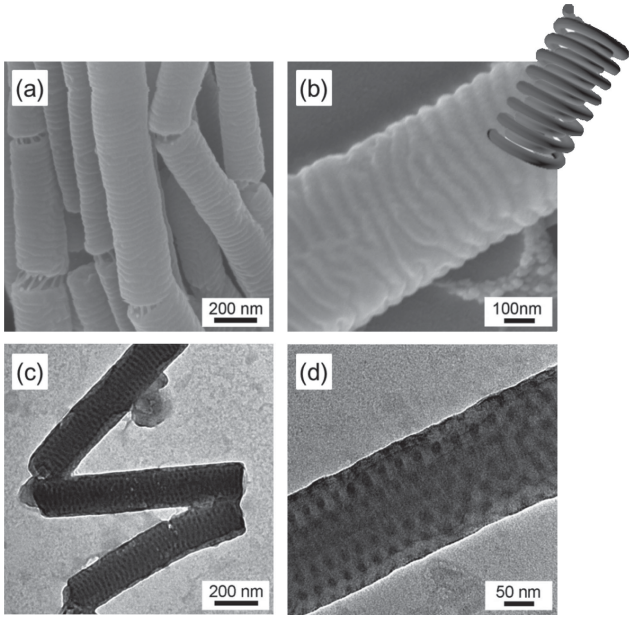

Figure 2. a,b) SEM images of PS-*b*-PDMS nanostructures: a) lower magnification and b) higher magnification. c,d) TEM images of PS-*b*-PDMS nanostructures: c) lower magnification and d) higher magnification. The samples are prepared by annealing the block copolymer films in co-solvent (toluene/hexane = 3:2) vapors for 24 h.

Hexane is a better solvent for the PDMS block than for the PS block. Using hexane as the annealing solvent, PS-*b*-PDMS is also found to wet the nanopores successfully, as shown in the SEM images (Figure S2a,b, Supporting Information). The cylindrical PDMS domain is observed to arrange irregularly in the nanopores (the irregular morphology). The irregular morphology is also confirmed by the TEM results (Figure S2c,d, Supporting Information).

To further control the morphologies of PS-*b*-PDMS nanostructures in the nanopores, a mixed solvent of toluene and hexane is used. Jung and Ross studied the morphologies changes of PS-*b*-PDMS thin films confined in 40 nm deep trenches and observed perforated lamellar morphologies when the thin films were annealed in co-solvent vapors with a ratio of 3:2 (toluene/heptane).[46] The molecular weights (31-*b*-14.5 kg mol^{-1}) and volume fractions (66.5-*b*-33.5%) of their PS-*b*-PDMS samples are similar to ours. But we use hexane in the co-solvent instead of heptane in our experiments. The SEM images of the PS-*b*-PDMS nanostructures annealed in co-solvent (toluene/hexane = 3:2, volume fraction) vapors are shown in Figure 2a,b. The cylindrical PDMS domains are arranged parallel to the curved AAO walls and similar to stacked rings (the circular morphology). The circular morphology is also confirmed in the TEM images (Figure 2c,d). Surprisingly, helical PDMS domains are also observed in some of the nanostructures.

In addition to the experiments using the co-solvent at a ratio of "toluene/hexane = 3:2", another co-solvent ratio (toluene/hexane = 4:2) is also used. Similar morphologies are observed in both conditions, as shown in Figure S3a,b (Supporting Information). More detailed studies using different solvent ratios might be necessary in the future to further understand the solvent-annealing-induced morphology change of the 3D block copolymers nanostructures.

The various morphologies of PS-*b*-PDMS nanostructures by annealing the samples in different solvent vapors are related to the solubility parameters, surface tensions, and interfacial tensions of polymers and solvents. The solubility parameters (δ) of toluene, PS, and PDMS are 18.2, 18.5, and 15.5 (MPa)$^{1/2}$, respectively.[44] Therefore, toluene has a preferential affinity to the major PS block and facilitates microphase separation of the block copolymers. The surface tension of PS is 40.7 mJ m^{-2}, which is higher than that of PDMS (19.9 mJ m^{-2}).[47] But the surface tensions of the two blocks can be mediated by the strong affinity of the annealing toluene vapors to the PS block, resulting in the formation of perpendicular morphologies, as shown in Figure 1. The balance between the polymer–solvent affinity and surface energy of the swollen blocks was also demonstrated previously in block copolymers thin films by Chuang et al.[48]

The solubility parameter of hexane is 14.9 (MPa)$^{1/2}$. Thus, hexane is not a good solvent for the major PS block and the microphase separation of the block copolymer is impeded, due to the limitation of the chain mobilities under hexane vapor annealing, as shown in Figure S2 (Supporting Information).[48] When the annealing solvent is changed to the co-solvent of toluene and hexane, the mobility of the major PS block is facilitated by the toluene vapors, allowing for microphase separation. The minor PDMS block is also swollen in the co-solvent vapors since hexane is a good solvent for PDMS. The difference of the surface tensions between the PS and PDMS blocks annealed in mixed-solvent vapors also causes the formation of the circular morphology, as shown in Figure 2.

One unique feature of this work is that the microphase separation of block copolymer nanostructures can be directly observed in the SEM images. For the block copolymer nanostructures studied in the past using template-based methods, the microphase separations are only observed in TEM images.[13–19] In SEM images, however, smooth surfaces are usually seen, due to the replication of the smooth walls in the AAO templates.

The appearance of the surface topography on the nanostructures is caused by the shrinkage of the PDMS domain after the AAO templates are removed. The glass transition temperatures (T_gs) of PS and PDMS are 100 and –121 °C, respectively. Since the T_g of PDMS is well below room temperature, the PDMS domains in the block copolymer nanostructures are rubbery at room temperature. After the AAO templates are removed by $NH_4OH_{(aq)}$, the residual

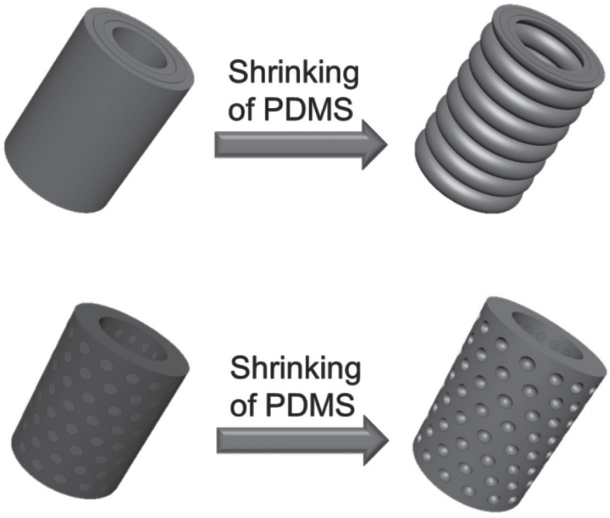

Figure 3. Graphical illustration of the shrinking process and the change of the surface morphologies of PS-*b*-PDMS nanostructures.

stress generated during the solvent-annealing wetting process may be dissipated by the rearrangement of the PDMS chains, resulting in the formation of wrinkled topography on the nanostructure surfaces. In addition to the dissipation of the residual stress, the appearance of the surface topography may be related to the different swelling ratios during the solvent-annealing process. After the annealing solvents are evaporated, the different degrees of shrinkage of the PS and the PDMS blocks may also cause the formation of the wrinkled topography on the nanostructure surfaces.

The formation model of the wrinkled topography is illustrated in Figure 3, assuming that the residual stress and the low T_g of the PDMS blocks are responsible for the formation of the surface topography. Before the removal of the AAO templates, the block polymers adhere to the AAO walls and smooth surfaces of the nanostructures are formed inside the nanopores. After the AAO templates are removed by $NH_4OH_{(aq)}$, the PDMS chains rearrange and cause the formation of different wrinkled topographies on the nanostructure surfaces. For the PS-*b*-PDMS nanostructures with the perpendicular morphology, the cylindrical PDMS domains shrink and cause the formation of the dimples on the nanostructure surfaces. For the PS-*b*-PDMS nanostructures with the circular morphology, the circular PDMS domains shrink and cause the formation of the stacked ring (or helices) on the nanostructure surfaces. The surface topography shown in this work reveals the microphase separation of the block copolymers, which is beneficial for characterizing the samples.

To further confirm the morphologies of the PS-*b*-PDMS nanostructures, 48 wt% HF solution is used to etch the PDMS domains selectively. Porous PS nanostructures are obtained after the etching process, as shown in Figure 4. For the PS-*b*-PDMS nanostructures with the perpendicular

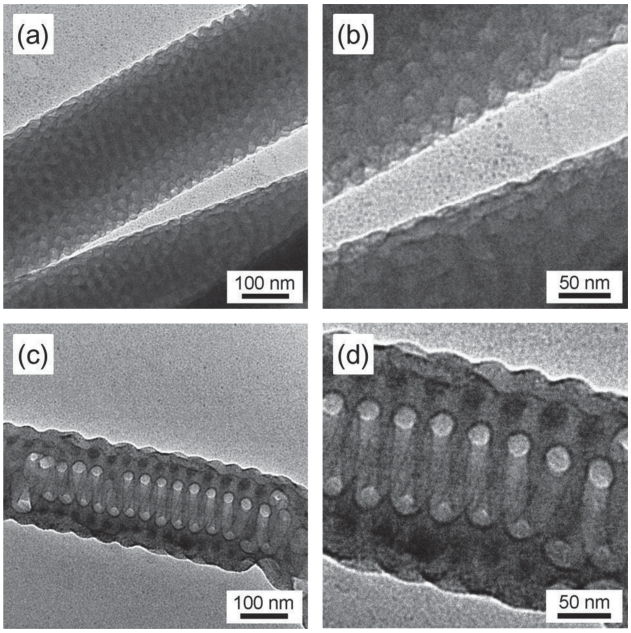

Figure 4. a,b) TEM images of porous PS nanostructures: a) lower magnification and b) higher magnification. The samples are first prepared by annealing the PS-*b*-PDMS films in toluene vapors, followed by an etching process using 48 wt% HF to remove selectively the PDMS block. c,d) TEM images of porous PS nanostructures: c) lower magnification an d d) higher magnification. The samples are first prepared by annealing the PS-*b*-PDMS films in co-solvent (toluene/hexane = 3:2) vapors, followed by an etching process using 48 wt% HF to remove selectively the PDMS block.

morphology by annealing in toluene vapors, the perpendicular PDMS domains are etched and appear lighter than the PS domains in the TEM images, as shown in Figure 4a,b. Similar results are also obtained by performing the selective etching processes while the AAO templates have already been removed (Figure S4, Supporting Information). Without the templates, the PDMS domains can be etched more effectively and the morphologies are easier to be determined.

The circular or helical PDMS domains in the PS-*b*-PDMS nanostructures with the circular morphologies by annealing in the co-solvent vapors can also be etched. Figure 4c,d shows the samples with partially removed PDMS domains using modest etching conditions, such as a shorter etching time (≈10 s). As a result, PDMS domains with and without etching can be observed in the same sample. As shown in Figure 4d, the inner helical PDMS domain is removed and appears lighter than the PS domain, while the outer PDMS domain is remained and appears darker than the PS domain. The selective removing process not only confirms the morphologies of the PS-*b*-PDMS nanostructures by the SAINT method, but also provides a facile route for fabricating novel nanostructures, which can be achieved by refilling the nanopores with other functional materials, such as Au, Ag, ZnO, and TiO_2.

An alternative to confirm the morphologies of the PS-*b*-PDMS nanostructures by the SAINT method is to perform the selective removing process using oxygen reactive ion etching (RIE). In the past, the oxygen RIE has been used in etching the PS domains of PS-*b*-PDMS thin films. It needs to be noted, however, that the selective removing process might be problematic for etching the nanostructures confined in the nanopores of the AAO templates. The PS-*b*-PDMS nanostructures are protected by the surrounding AAO walls, and the reactive ions may be largely blocked by the templates, resulting in the incomplete removal of the PS domains. By comparison, the selective removal process using HF solutions is considered to be more effective since the HF solutions can wet and etch the confined nanostructures via capillary force.

4. Conclusion

We successfully prepare PS-*b*-PDMS nanostructures using solvent-annealing-induced wetting in porous AAO templates. Different from the traditional melt method, heating is not involved in the annealing process and the problem of thermal degradation is avoided. The morphologies of the block copolymer nanostructures can be controlled by the type of the annealing solvent. The perpendicular morphology can be obtained by annealing the sample in toluene vapors, while an irregular morphology is obtained by annealing the sample in hexane vapors. By annealing the sample in mixed solvent vapors (toluene/hexane = 3:2), the circular morphology can be observed, where circular or helical PDMS domains are formed. These different morphologies are also confirmed from the porous PS nanostructures by etching the PDMS domain selectively. In the future, we will refill the nanopores in the PS nanostructures with metal or inorganic materials using techniques such as atomic layer deposition (ALD) or the sol–gel process. The obtained circular or helical metal nanostructures may have interesting electronic or optical properties, such as the plasmonic effect.

Supporting Information

Supporting Information is available from the Wiley Online Library or from the author.

Acknowledgements: This work was supported by the Ministry of Science and Technology of the Republic of China.

Received: April 14, 2014; Revised: June 4, 2014; Published online: August 7, 2014; DOI: 10.1002/marc.201400222

Keywords: block copolymers; self-assembly; solvent annealing; template; wetting

[1] I. W. Hamley, *Nanotechnology* **2003**, *14*, R39.
[2] G. Riess, *Prog. Polym. Sci.* **2003**, *28*, 1107.
[3] M. P. Stoykovich, P. F. Nealey, *Mater. Today* **2006**, *9*, 20.
[4] R. A. Segalman, B. McCulloch, S. Kirmayer, J. J. Urban, *Macromolecules* **2009**, *42*, 9205.
[5] J. T. Chen, C. S. Hsu, *Polym. Chem.* **2011**, *2*, 2707.
[6] M. L. Adams, A. Lavasanifar, G. S. Kwon, *J. Pharm. Sci.* **2003**, *92*, 1343.
[7] F. S. Bates, G. H. Fredrickson, *Annu. Rev. Phys. Chem.* **1990**, *41*, 525.
[8] M. J. Fasolka, A. M. Mayes, *Annu. Rev. Mater. Res.* **2001**, *31*, 323.
[9] Y. Y. Wu, G. S. Cheng, K. Katsov, S. W. Sides, J. F. Wang, J. Tang, G. H. Fredrickson, M. Moskovits, G. D. Stucky, *Nat. Mater.* **2004**, *3*, 816.
[10] B. Yu, P. C. Sun, T. H. Chen, Q. H. Jin, D. T. Ding, B. H. Li, A. C. Shi, *Phys. Rev. Lett.* **2006**, *96*, 138306.
[11] A. C. Shi, B. H. Li, *Soft Matter* **2013**, *9*, 1398.
[12] H. Yabu, T. Higuchi, H. Jinnai, *Soft Matter* **2014**, *10*, 2919.
[13] K. Shin, H. Q. Xiang, S. I. Moon, T. Kim, T. J. McCarthy, T. P. Russell, *Science* **2004**, *306*, 76.
[14] H. Q. Xiang, K. Shin, T. Kim, S. I. Moon, T. J. McCarthy, T. P. Russell, *Macromolecules* **2004**, *37*, 5660.
[15] H. Xiang, K. Shin, T. Kim, S. I. Moon, T. J. McCarthy, T. P. Russell, *Macromolecules* **2005**, *38*, 1055.
[16] H. Q. Xiang, K. Shin, T. Kim, S. Moon, T. J. McCarthy, T. P. Russell, *J. Polym. Sci., Part B: Polym. Phys.* **2005**, *43*, 3377.
[17] P. Dobriyal, H. Q. Xiang, M. Kazuyuki, J. T. Chen, H. Jinnai, T. P. Russell, *Macromolecules* **2009**, *42*, 9082.
[18] Y. M. Sun, M. Steinhart, D. Zschech, R. Adhikari, G. H. Michler, U. Gosele, *Macromol. Rapid Commun.* **2005**, *26*, 369.
[19] Y. Wang, U. Goesele, M. Steinhart, *Chem. Mater.* **2008**, *20*, 379.
[20] A. M. M. Jani, D. Losic, N. H. Voelcker, *Prog. Mater. Sci.* **2013**, *58*, 636.
[21] H. Masuda, K. Fukuda, *Science* **1995**, *268*, 1466.
[22] A. P. Li, F. Muller, A. Birner, K. Nielsch, U. Gosele, *J. Appl. Phys.* **1998**, *84*, 6023.
[23] O. Jessensky, F. Muller, U. Gosele, *Appl. Phys. Lett.* **1998**, *72*, 1173.
[24] M. Steinhart, J. H. Wendorff, A. Greiner, R. B. Wehrspohn, K. Nielsch, J. Schilling, J. Choi, U. Gosele, *Science* **2002**, *296*, 1997.
[25] M. Steinhart, R. B. Wehrspohn, U. Gosele, J. H. Wendorff, *Angew. Chem. Int. Edit.* **2004**, *43*, 1334.
[26] M. F. Zhang, P. Dobriyal, J. T. Chen, T. P. Russell, J. Olmo, A. Merry, *Nano Lett.* **2006**, *6*, 1075.
[27] P. G. Degennes, *Rev. Mod. Phys.* **1985**, *57*, 827.
[28] V. M. Cepak, C. R. Martin, *Chem. Mater.* **1999**, *11*, 1363.
[29] J. T. Chen, K. Shin, J. M. Leiston-Belanger, M. F. Zhang, T. P. Russell, *Adv. Funct. Mater.* **2006**, *16*, 1476.
[30] J. T. Chen, M. F. Zhang, L. Yang, M. Collins, J. Parks, A. Avallone, T. P. Russell, *J. Polym. Sci. Part B: Polym. Phys.* **2007**, *45*, 2912.
[31] J. T. Chen, M. F. Zhang, T. P. Russell, *Nano Lett.* **2007**, *7*, 183.
[32] D. Chen, J. T. Chen, E. Glogowski, T. Emrick, T. P. Russell, *Macromol. Rapid Commun.* **2009**, *30*, 377.
[33] C. C. Tsai, J. T. Chen, *Langmuir* **2014**, *30*, 387.
[34] T. C. Wang, H. Y. Hsueh, R. M. Ho, *Chem. Mater.* **2010**, *22*, 4642.
[35] S. L. Mei, X. D. Feng, Z. X. Jin, *Soft Matter* **2013**, *9*, 945.
[36] J. T. Chen, C. W. Lee, M. H. Chi, I. C. Yao, *Macromol. Rapid Commun.* **2013**, *34*, 348.
[37] E. Helfand, Y. Tagami, *J. Chem. Phys.* **1972**, *56*, 3592.

[38] I. F. Hsieh, H. J. Sun, Q. Fu, B. Lotz, K. A. Cavicchi, S. Z. D. Cheng, *Soft Matter* **2012**, *8*, 7937.
[39] J. G. Son, J. B. Chang, K. K. Berggren, C. A. Ross, *Nano Lett.* **2011**, *11*, 5079.
[40] K. W. Gotrik, A. F. Hannon, J. G. Son, B. Keller, A. Alexander-Katz, C. A. Ross, *ACS Nano* **2012**, *6*, 8052.
[41] J. B. Chang, J. G. Son, A. F. Hannon, A. Alexander-Katz, C. A. Ross, K. K. Berggren, *ACS Nano* **2012**, *6*, 2071.
[42] M. L. Wadey, I. F. Hsieh, K. A. Cavicchi, S. Z. D. Cheng, *Macromolecules* **2012**, *45*, 5538.
[43] B. A. Miller-Chou, J. L. Koenig, *Prog. Polym. Sci.* **2003**, *28*, 1223.
[44] J. Brandrup, E. H. Immergut, E. A. Grulke, *Polymer Handbook*, 4th ed., Wiley, New York **1999**.
[45] T. Hashimoto, M. Shibayama, H. Kawai, *Macromolecules* **1983**, *16*, 1093.
[46] Y. S. Jung, C. A. Ross, *Adv. Mater.* **2009**, *21*, 2540.
[47] K. A. Cavicchi, K. J. Berthiaume, T. P. Russell, *Polymer* **2005**, *46*, 11635.
[48] V. P. Chuang, C. A. Ross, J. Gwyther, I. Manners, *Adv. Mater.* **2009**, *21*, 3789.